

The copper atoms in the second set of 32:(*f*) positions have thirteen atoms in the first coordination polyhedron. Three magnesium atoms, four silicon atoms, and six copper atoms are at the vertices of this polyhedron, which is related to the icosahedron.

The interatomic distances are given in Table 3. In this table bond numbers as well as calculated valences of the various atoms are also given, as calculated using the relation

$$R(1) - R(n) = 0.300 \log n,$$

when  $R$  is the metallic radius and  $n$  the bond number (Pauling, 1947).

The positional parameters given by Nagorsen & Witte (1953), after change of origin, are included in Table 1. Only the magnesium atoms are given substantially different positions in the two investigations. The incomplete table of interatomic distances given by Nagorsen & Witte does not show to what extent the packing is unsatisfactory if their parameter is assumed correct. The Mg-Mg distances turn out to be 3.50 Å, as compared to 2.99 Å in this investigation. Also the rather large holes at (0, 0, 0) etc. appear difficult to explain. The long Mg-Mg distances are also unlikely in view of the results obtained by Florio, Rundle & Snow (1952) for the binary phase Th<sub>6</sub>Mn<sub>23</sub>. This phase has the same general arrangement of the atoms in the unit cell. The Th atoms take the place of the Mg atoms and the Mn atoms take the place of the Cu and Si atoms. The Th<sub>6</sub>Mn<sub>23</sub> structure may therefore be considered as a special case of the more

general  $A_6B_7C_{16}$  type structure described here.† The Th-Th distance is 3.59 Å and the metallic radius of the thorium atom for coordination twelve is 1.795 Å (Pauling, 1947).

We acknowledge with gratitude the financial support of the Office of Naval Research, which sponsored the work under a contract with this Institute. We also wish to thank Prof. Linus Pauling for suggesting the problem.

#### References

- BERGMAN, G. & WAUGH, J. L. T. (1953). *Acta Cryst.* **6**, 93.  
 CROUT, P. D. (1941). *Elect. Engng.*, N.Y. **60**, 1235.  
 FLORIO, J. V., RUNDLE, R. E. & SNOW, A. I. (1952). *Acta Cryst.* **5**, 449.  
 HUGHES, E. W. (1941). *J. Amer. Chem. Soc.* **63**, 1737.  
*Internationale Tabellen zur Bestimmung von Kristallstrukturen* (1935). Berlin: Borntraeger.  
 LANGE, J. J. DE, ROBERTSON, J. M. & WOODWARD, I. (1939). *Proc. Roy. Soc. A*, **171**, 398.  
 NAGORSEN, G. & WITTE, H. (1953). *Z. anorg. Chem.* **271**, 144.  
 PAULING, L. (1947). *J. Amer. Chem. Soc.* **69**, 542.  
 ROBERTSON, J. M. (1943). *J. Sci. Instrum.* **20**, 175.  
 WITTE, H. (1938). *Z. angew. Min.* **1**, 255.

† The paper by Florio *et al.* appeared in print after the work described here had been finished, with the exception of the last refinement. The atomic arrangement described has consequently been discovered by three independent groups of investigators.

*Acta Cryst.* (1956). **9**, 217

## Growth Features on Crystals of Long-Chain Compounds. III

BY S. AMELINCKX

*Laboratorium voor Kristalkunde, Rozier 6, Gent, Belgium*

(Received 24 May 1955)

Interlaced patterns have been observed on a monoclinic form of the paraffin C<sub>34</sub>H<sub>70</sub>, on behenic acid and on the  $\alpha$ -form of the  $n$ -alcohols C<sub>34</sub>H<sub>47</sub>OH. The patterns are analysed using the method outlined in Part I, and deductions are made concerning the stacking sequences of the crystals on which they are observed. It is found that in crystals of tetratriacontane and behenic acid successive growth layers can be turned through 180°, and that this kind of stacking fault is responsible for the growth of polytypic crystals. It is further shown that growth round *imperfect* dislocations in behenic acid *does not produce polytypes*, but that, on the contrary, the normal structure is continued.

An interlaced pattern, observed on a crystal of the  $\alpha$ -form of the  $n$ -alcohols, is also interpreted in terms of the stacking of successive layers. This pattern is the first example of a 'doubly interlaced pattern', i.e. an interlacing of two patterns which are themselves interlaced.

### 1. General introduction

In Part I of this series of papers we have discussed a method of obtaining information concerning the

stacking of polytypic crystals from the interlaced patterns observed on them. The method was illustrated by means of patterns observed on crystals of the  $\beta$ -form of the  $n$ -alcohols. In this third paper we will

apply it to three somewhat simpler cases, i.e. to the *B*-form of the monocarboxylic acids (eicosanic, behenic and lignoceric acids), to a monoclinic form of the *n*-paraffins, and to the  $\alpha$ -form of the *n*-alcohols.

Observations were made with phase contrast in reflexion; step heights were measured by means of multiple-beam interferometry (Tolansky, 1948); the crystals were silvered on both sides.

## 2. Growth features on crystals of the *n*-paraffin $C_{34}H_{70}$ (monoclinic form)

### 2.1. Introduction

The spiral growth (Frank, 1949) of *n*-paraffin crystals has been studied by means of the electron microscope by Dawson *et al.* (Dawson & Vand, 1951; Dawson, 1952; Anderson & Dawson, 1953). They studied the *n*-paraffins  $C_{36}H_{74}$ ,  $C_{39}H_{80}$  and  $C_{100}H_{202}$ , which invariably crystallized in the orthorhombic form. No reference was made either to interlaced spirals or to polytypism. These properties are strikingly presented by the lower members of the *n*-paraffins. They are also of interest because they exhibit a more pronounced polymorphism (Mazee, 1948). By means of phase-contrast microscopy we have studied the *n*-paraffin  $C_{34}H_{70}$ , of which a sample was kindly supplied to us by Prof. Stenhagen. This paraffin is known to crystallize in at least two polymorphs: the orthorhombic form with  $a = 7.40$ ,  $b = 4.95$  Å (Müller, 1928, 1932), and the monoclinic form with  $a = 5.58$ ,  $b = 7.48$  Å (Dawson & Vand, 1951).

The two polymorphs are thus easily distinguished by means of the acute angle  $\chi$  of the lozenge-shaped crystal plate delimited by [110] edges;  $\chi$  can be calculated from the lattice parameters and its value is  $67^\circ$  and  $74^\circ$  for the orthorhombic and the monoclinic modifications respectively. It is further known that the unit cell for *n*-paraffins containing an even number of carbon atoms in the chain is one monolayer high for both forms.

### 2.2. Shape of elementary spirals

We will not discuss growth features on orthorhombic crystals as this subject has been treated in detail by Dawson *et al.*

Very small crystals were obtained at room temperature from benzene and xylene. They were generally of the monoclinic form with  $\chi = 74^\circ$ ; this angle is subject to slight variations; values between  $72^\circ$  and  $76^\circ$  were noted.

In general the growth steps were monomolecular, in accordance with the observations of Dawson *et al.* on orthorhombic crystals. The shape of the spirals is as shown in Fig. 1. A constant feature is the inequality of the spacings in two halves of the crystal face. The growth pattern has consequently only a plane (a line) of symmetry along the short diagonal of the lozenge. This is in accordance with the monoclinic cell as deduced from the X-ray measurements; the short

diagonal is the trace of the *b* plane, which is also the plane of tilt of the chains. The polar diagram for the growth velocity, as deduced from the shape of these spirals, is represented schematically in Fig. 10; its symmetry (*P*) is  $1m$ . There are in general four minima corresponding to the directions normal to the [110] edges. The two deepest are called (*a*); the others (*b*). The ratio  $v_b/v_a$  can be deduced from the value of the acute angle  $\gamma$  between the two parts of the long diagonal:

$$v_b/v_a = \sin \frac{1}{2}(\alpha + \gamma) / \sin \frac{1}{2}(\alpha - \gamma).$$

Values for  $\gamma$  of the order of  $15^\circ$  are observed: i.e.  $v_b/v_a \approx 1.5$ .

### 2.3. Stacking possibilities of monolayers

The upper and lower surfaces of a monolayer of paraffin molecules consist of two-dimensional lattices of  $CH_3$  groups. This two-dimensional pattern has to a first approximation a twofold axis of symmetry perpendicular to the *c* plane. As a consequence it is to be expected that two similar layers can be stacked without appreciable misfit in two different ways: either in the normal way, i.e. the chains being parallel in successive layers; or in such a way that successive layers are turned one with respect to the other through  $180^\circ$  about an axis normal to *c*(001). We do not consider here the stacking differences which could result from the presence of two kinds of hollows:  $\Delta$  and  $\nabla$  hollows (Frank, 1951).

Using the terminology of Part I (Amelinckx, 1955) we say that the 'allowed' rotations are  $\varphi = k \times 180^\circ$  or that the stacking symmetry *S* corresponds to the plane point group 2.

As *S* is not a subgroup of *P*, two different growth patterns are to be expected: one corresponding to the normal stacking, and one to the stacking of layers which are turned relatively through  $180^\circ$ .

When representing a monolayer by the symbol *A* (which has a line of symmetry) stacking sequences can be described by giving a sequence of symbols like  $A \nabla \dots$  or  $A A A \nabla \nabla \dots$ , the normal stacking being  $A \dots$ . It is also possible to introduce a numerical symbol indicating the number of layers in each position: e.g. 11, 32,  $\dots$ .

### 2.4. Interlaced patterns and polytypism

Apart from the simple spirals described above, in a relatively great number of cases (5–10%) interlaced patterns of the shape represented by Figs. 2 and 10 were observed.

Applying the procedure for the analysis of interlaced spirals, outlined in Part I, it is found that the spiral of Fig. 10 can be decomposed into two elementary spirals, as shown on the same figure.

The following set of inequalities can be deduced from it:

$$\begin{array}{ll} {}^1v_B \leq {}^1v_A, & {}^3v_A \leq {}^3v_B, \\ {}^2v_A < {}^2v_B, & {}^4v_B < {}^4v_A. \end{array}$$



Fig. 1. Elementary monomolecular spiral on crystal of the monoclinic form of tetratriacontane ( $C_{34}H_{70}$ ) (900 $\times$ ).

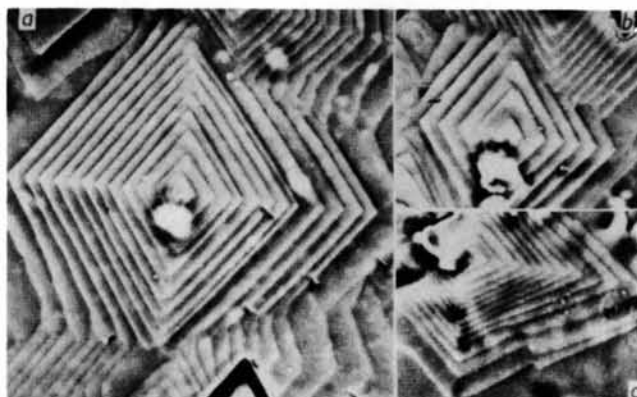


Fig. 3. Interlaced spirals on polytypic crystals of the monoclinic form of tetratriacontane (800 $\times$ ). Structure symbols: (a)  $AAV\bar{V}$  (22); (b)  $AAAAV\bar{V}$  (32); (c)  $AAV$  (21).

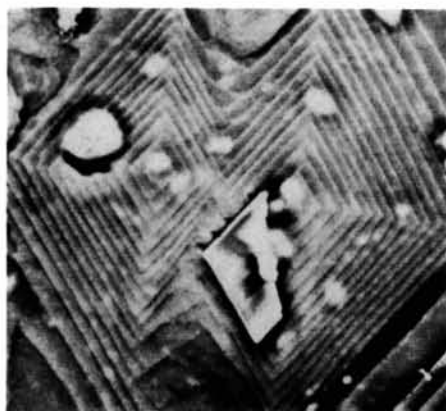


Fig. 2. Two interlaced spirals on polytypic crystal of the monoclinic form of tetratriacontane. The structure symbol of the polytype is  $AV$  (or 11) (850 $\times$ ).

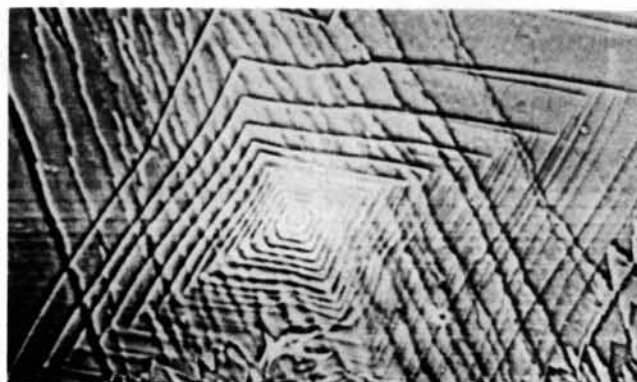


Fig. 4. Complicated interlaced spiral on crystal of  $C_{34}H_{70}$  (monoclinic form) (600 $\times$ ).

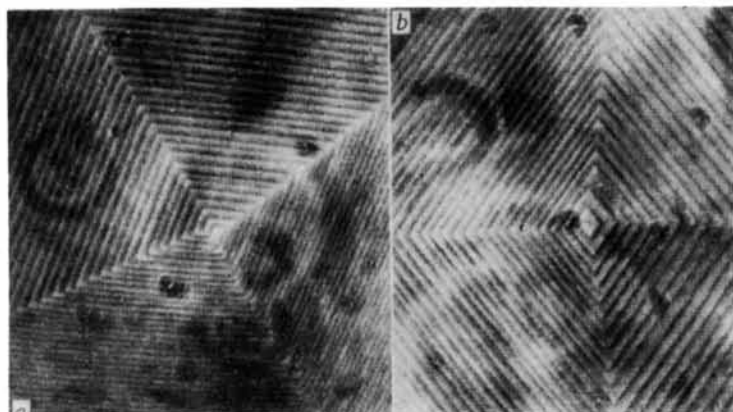


Fig. 5. (a) Elementary spiral on crystal of the *B*-form of behenic acid (1300×). (b) Two spirals of opposite sign on crystal of the *B*-form of behenic acid (650×).

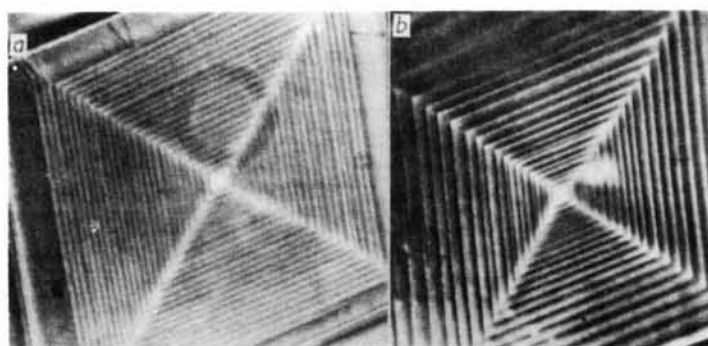


Fig. 6. Interlaced spirals on polytypic crystal of behenic acid (interlacings in the acute angles). Structure symbols: (a)  $A\vee$  (750×); (b)  $AA\vee\vee$  (750×).

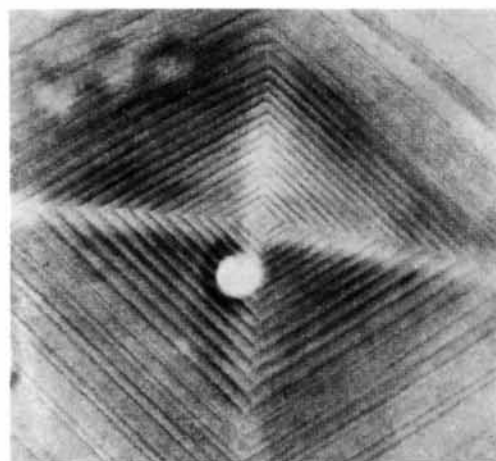


Fig. 7. Interlaced spiral (cross-lacing in one obtuse angle). The pattern is due to growth round an imperfect dislocation (800×).

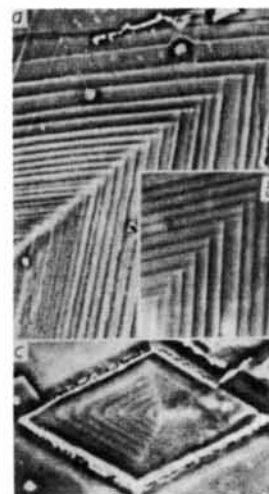


Fig. 8. Behenic acid: (a, b) Interlaced patterns on polytypic crystals. Structure symbol  $AA\vee$  (750×). (c) Elementary spiral on crystal of the *C*-form (600×).



Fig. 9. Interlaced spiral on crystal of *n*-alcohol ( $C_{24}H_{47}OH$ ). Cross-lacings in the four corners (800×).

By means of the polar diagram (Fig. 10), deduced in § 2.2, it can be shown that the layers *A* and *B* corresponding to the two spirals are to be turned 180° one with respect to the other in order to satisfy all the inequalities. The polar diagrams for *A* and *B* are drawn in their hypothetical orientations in Fig. 10. It is easy to verify that interlacing is obtained in the acute angles, in accordance with observation. Moreover, the spacings are now equal in the four sectors, as they are all determined by  $v_a$ ; this is also consistent with the observations.

It is thus concluded that the stacking sequence of the crystal of Fig. 2 should be  $A \nabla$  (or 11). This follows from the monomolecular character of the steps of the component spirals *A* and *B*. We observed however patterns where this was not the case. Fig. 3(a) gives an example where both component spirals have bimolecular fronts. This is deduced in a very simple way from the fusion of fronts in the region of the acute angles. It is directly evident that two fronts of spiral 1 have the same height as one front of spiral 2. The structure of the crystal is consequently (22).

Fig. 3(b) shows another example; from the fusion of growth steps with those of the simple interlaced spiral it is evident that  $2\frac{1}{2}$  fronts of the simple interlaced spiral have the same height as one front of the central spiral, so that the main fronts are five molecules high. As the interlacing growth steps have approximately the same height it is justified to suppose that one is three and the other two molecules high; the corresponding structure would be  $AA A \nabla \nabla$  (or 32).

Fig. 3(c) shows, on the other hand, a spiral where the main steps are three molecules high. This can be deduced from the grouping of fronts near the centre. The 'cross-lacing' fronts are now necessarily one and two molecules high and the corresponding structure of the crystal is  $AA A \nabla$  (or 21).

Other examples, where the 'cross-lacing' steps are not elementary, were observed. No definite conclusion could be drawn concerning step heights; in one case the main steps were 7 or 8 molecules high and the structure symbol probably 43 or 53.

We can now generalize. A crystal having the structure  $(AA \dots A)_m (\nabla \nabla \dots \nabla)_n$  will exhibit a spiral having main growth fronts  $m+n$  monolayers high, and the cross-lacing steps will be  $m$  and  $n$  monolayers high.

The structure of the crystal can thus be deduced directly from the heights  $m$  and  $n$  of the cross-lacing steps. The steps  $m$  and  $n$  may in some cases be dissociated.

Where the  $c$  period of the crystal contains more than two differently oriented lamella (this number is necessarily even!), e.g.

$$(AA \dots A)_p (\nabla \nabla \dots \nabla)_q (AA \dots A)_m (\nabla \nabla \dots \nabla)_n,$$

the spiral will in general separate into a multiple interlaced spiral with main fronts in one half having successively heights of  $m+n$  and  $p+q$ , and in the other half  $n+p$  and  $q+m$ ; the interlacing growth steps being  $m, n, p$  and  $q$  respectively.

No well formed spiral of this kind was observed, but Fig. 4 gives an example where the separation into a multiple interlaced spiral is not complete. In the two acute angles of the lozenge the growth fronts are grouped in a characteristic way. The same way of grouping is repeated several times in a given angle; moreover, the periodicity is the same in the two acute angles; this suggests that a real significance is to be attached to it. It is thought that this spiral originates in a complicated polytype having a repeat distance of at least the height of 8 monolayers.

In Table 1 we have summarized the characteristics of a number of observed polytypes.

### 2.5. Miscellaneous growth features

The equality of the angle  $\chi$  for the crystals of the monoclinic  $n$ -paraffin, here described, and of crystals of the form *B* of monocarboxylic acids suggests that the structure of the limiting surfaces of  $\text{CH}_3$  groups will be the same in both cases. That this is in fact so is supported by the similarity of the polytypism of both compounds (see further). It is further confirmed by the occurrence of twins of the same type as those described in Part II (Amelinckx, 1956), for the monocarboxylic acids (form *B*).

## 3. Growth features on crystals of monocarboxylic acids

### 3.1. Introduction

We have studied three long-chain acids: eicosanic, behenic and lignoceric acids. Some preliminary results have already been published (Amelinckx, 1953, 1954).

Table 1. Polytypes of monoclinic form of  $n$ -paraffin,  $\text{C}_{34}\text{H}_{70}$

Symmetry class	Number of monolayers in unit cell	Structure symbols	Number of times observed	Fig.
Monoclinic	1	A	*	1
Orthorhombic	2	$A \nabla$	11	2
Monoclinic	3	$AA \nabla$	21	3(c)
Orthorhombic	4	$AA \nabla \nabla$	22	3(a)
Monoclinic	5	$AAA \nabla \nabla$	32	3(b)
Monoclinic	8	—	1	4
Monoclinic	7 or 8	—	1	—

\* Normal stacking.

As, apart from the step height, no specific differences were observed between the growth features on these three substances, the main effort was concentrated on behenic acid.

Stearic acid has already been studied in some detail by Anderson & Dawson (1953), and also by Verma & Reynolds (1953). Recently Verma (1955) has published also a study on the growth of palmitic acid.

On crystals of the three acids mentioned above, some features were observed which were not described by the previous authors; this justifies their publication here.

We prepared our crystals by the slow evaporation of solutions on object glasses. Benzene and xylene as solvents gave the best results. Crystallization always yielded a mixture of crystals of the forms *B* and *C* described by Piper, Malkin & Austin (1926). They can easily be distinguished by means of the acute interfacial angles of the lozenge-shaped crystals; they are  $\chi = 74^\circ$  for *B* and  $\chi = 56^\circ$  for *C*. The great majority of the crystals were of form *B* in our crystallizations, so that the observations were nearly exclusively made on crystals of this modification. A higher crystallization temperature seems to favour the appearance of the form *C*.

### 3.2. Shape of elementary spirals on crystals of the form *B*

In most cases the fronts are bimolecular; the growth pattern has only a line of symmetry (symmetry class:  $1m$ ) indicating the trace of the *b* plane, which is along the short diagonal. This is clearly visible in Fig. 5(a) and (b), where the two parts of the long diagonal form an acute angle  $\gamma$  (cf. § 2.2). The value of  $\gamma$  ranges from  $0^\circ$  to some  $12^\circ$ , i.e.  $1 < v_b/v_a < 1.4$ . The symmetry of the pattern is thought to result, as in the

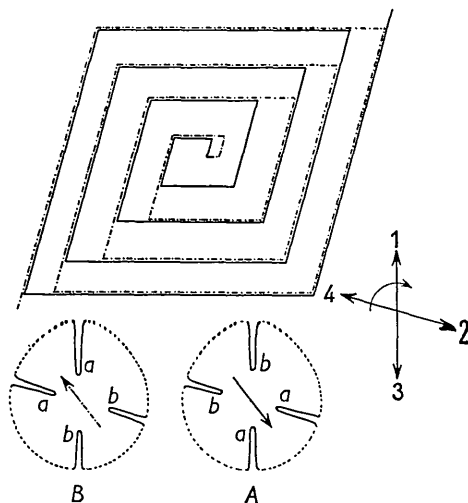


Fig. 10. Decomposition of interlaced spiral observed on the monoclinic form of the *n*-paraffins  $C_{34}H_{70}$  and on the *B*-form of the monocarboxylic acids. Cross-lacing steps in the acute angles. The polar diagrams of the two layers are also represented.

case of the *n*-paraffins, from the tilt of the chains.

The polar diagram for the growth velocity of a bimolecular layer can be represented qualitatively by Fig. 10, already used for the *n*-paraffins.

### 3.3. Stacking possibilities of bimolecular layers

Again we will not consider the stacking possibilities which result from the two families of hollows ( $\Delta$  and  $\nabla$ , Frank, 1951) which are available on a surface of  $CH_3$  groups. We also suppose that no stacking faults occur in the planes of the  $COOH$  groups.

The angle  $\chi$  being  $74^\circ$ , as in the case of the *n*-paraffins (§ 2.1), the geometry of the limiting plane of  $CH_3$  groups will be very approximately the same. We therefore have the same stacking possibilities, and the same sequences as deduced in § 2.3 are possible (the symbol *A* represents now a bimolecular layer).

### 3.4. Interlaced spirals and polytypism

In some cases interlaced patterns were observed on crystals grown from benzene. Examples are shown in Figs. 6(a), 6(b), 8(a) and 8(b). Interlacing takes place in the acute angles.

In the simple case of Fig. 6(a) the main fronts are four molecules high and the interlacing steps are consequently bimolecular. The interpretation of the pattern is quite simple, as it is completely similar to the one for the monoclinic form of the paraffins. The stacking sequence of the polytypic crystal on which this pattern was observed is consequently  $A \nabla$ .

As in the case of the *n*-paraffins, more complicated stacking sequences are to be expected and were in fact observed. Figs. 8(a) and 8(b) give examples of spirals for which the periodicity in the *c* direction is some  $170 \text{ \AA}$  (i.e. six molecules high). The cross-lacing fronts are thus 2 and 1 bimolecular layers thick, and the structure symbol of the crystal is in this case  $A A \nabla$ .

Another example is visible in Fig. 6(b). The main steps are now eight molecules high. As the cross-lacing steps are visibly equal, they are both four molecules high. The stacking symbol which can be deduced from this is  $A A \nabla \nabla$ .

We summarize in Table 2 the characteristics of the polytypes found for behenic acid.

### 3.5. Interlaced patterns and imperfect dislocations

Apart from the interlaced spirals described in § 3.4, we observed in some cases spirals with 'cross-lacings' in one of the obtuse angles; an example is shown in Fig. 7. In the central region the spiral is simple, but after some three turns the fronts dissociate and interlacing takes place in *only one* of the obtuse angles. This is a quite striking feature. From the relation derived in § 4.4 (Part I) it will be clear that the spiral cannot consist of an even number of branches. When following one front in the interlaced region of the spiral, it is found that after one complete turn the same front is three steps higher (or lower). This means

Table 2. *Polytypes of behenic acid*

Symmetry class	Number of bimolecular layers in unit cell	Stacking symbols		Number of times observed	Fig.
Monoclinic	1	A...	1	*	5(a), 5(b)
Orthorhombic	2	A V...	11	5	6(a)
Monoclinic	3	A A V...	21	2	8(a), 8(b)
Orthorhombic	4	A A V V...	22	1	6(b)

\* Normal stacking.

that at least three separately growing fronts are present. On elucidation the decomposition of Fig. 11 is obtained.

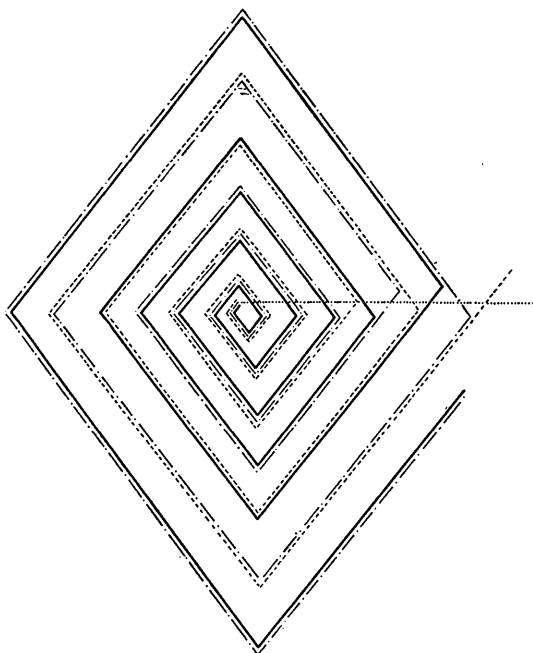


Fig. 11. Decomposition of interlaced spiral on crystal of the *B*-form of behenic acid. Cross-lacing in *one* of the obtuse angles.

From this decomposition it will be clear that a given front is rate-determining (i.e. slow) in a certain sector for one turn, but for the next turn the same front is fast in the same sector. This is true for all fronts in all sectors. This behaviour is characteristic of growth in the presence of an imperfect dislocation, when the substrate dictates the stacking (and not the exposed edge of the dislocation). This was already shown in detail in § 2.2 of Part II for the case of the  $\alpha$ -form of the *n*-alcohols. Imperfect dislocations of the same kind can be considered in crystals of the monocarboxylic acids. A change in stacking will have to take place every time the growth front crosses the misfit line as the front growing on a  $\text{CH}_3\text{-CH}_3$  bond will always be slow. To explain the pattern of Fig. 7 (or Fig. 11) the misfit line should, as a consequence, be somewhere along the short diagonal. The nearly undeformed step on the underneath face is in fact visible, and it is

even continuing as a non-growing step on the upper face. It is not a coincidence that the step is along the short diagonal, as the *b* plane is a glide plane. The original step was possibly straight (cf. Fig. 6 of Part II; here the step is along the long diagonal and along the short diagonal or just 'before' it (in the sense of winding of the spiral); subsequent growth has somewhat deformed it. Its hypothetical original position is indicated in Fig. 11.

From these arguments it will be clear that in the monocarboxylic acids, as in the *n*-alcohols, the orientation 'up' or 'down' of a molecule in the exposed edge will be determined by the substrate, rather than by the exposed edge. Polytypism due to imperfect dislocations is thus not to be expected. As shown above, polytypism implies stacking faults in these substances. This conclusion is at variance with that reached by Verma (1955).

#### 4. Growth features on crystals of monocarboxylic acids, *C*-form ( $\chi = 56^\circ$ )

##### 4.1. Shape of elementary spirals

The elementary spirals have bimolecular steps (Fig. 8(c)). There is again a line of symmetry along the trace of the *b* plane, which contains the tilt chains. This trace is now along the long diagonal, as in the case of the  $\beta$ -form of the *n*-alcohols (Part I). The long diagonal is consequently a line of symmetry for the polar diagram (*P* is *1m*).

##### 4.2. Stacking possibilities

The stacking possibilities are the same as in the two previous cases: *S* contains the rotations  $\varphi = k \times 180^\circ$ ; (*S* is 2).

##### 4.3. Interlaced patterns and polytypism

On the small number of crystals which could be investigated no interlaced patterns were found, probably because no polytypic crystals were present. We can, however, foresee that crystals with stacking sequences similar to those found for the *B*-form will occur, and we can tell what the growth pattern will look like. From the polar diagram and from the stacking symmetry, we have to expect interlacings in the two obtuse angles for crystals having a stacking sequence A V.

### 5. Discussion

An essential point in our analysis was the argument that the difference between the minima (a) and (b) of the polar diagram of Fig. 10 is due to the tilt of the chains. That this hypothesis is reasonable follows from the fact that in all four cases studied hitherto, of crystals growing with layers limited by  $\text{CH}_3$  groups, the line of symmetry is along the  $b$  plane, or the plane of tilt of the chains. This is in fact the case for: (i) the  $\beta$ -form of the  $n$ -alcohols (see Part I), (ii) the monoclinic form of the  $n$ -paraffins, (iii) the  $B$ -form of the mono carboxylic acids, (iv) the  $C$ -form of the monocarboxylic acids.

The difference in velocity for (a) and (b) minima

may be understood in the following way (see Fig. 12). For one family of fronts the molecules have to be attached to the crystal in an acute angle, whereas for the other family the angle is obtuse (Fig. 12). It is to be expected that the fronts where the angle is acute will be slow, as the arrival of molecules from the solution will have to take place over a smaller solid angle than for the other fronts.

Another argument supports the hypothesis: the difference in velocity for (a) and (b) fronts increases with increasing tilt angle  $\beta$  (see Fig. 12(a)). The anisotropy is small for the  $B$ -form of monocarboxylic acids, where the tilt angle is small, but it is much greater for the  $\beta$ -form of the  $n$ -alcohols, where the tilt angle is greater.

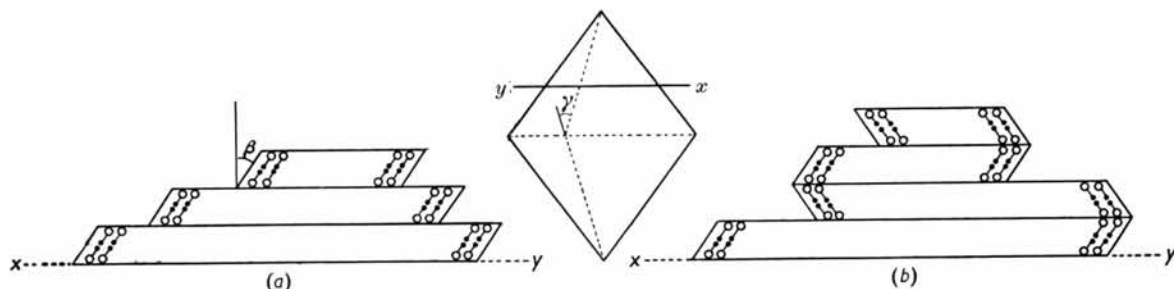


Fig. 12. Cut through a crystal of the  $B$ -form of the monocarboxylic acids to show the inclination of the chains in the growth fronts. (a) Normally stacked crystal; (b) polytypic crystal.

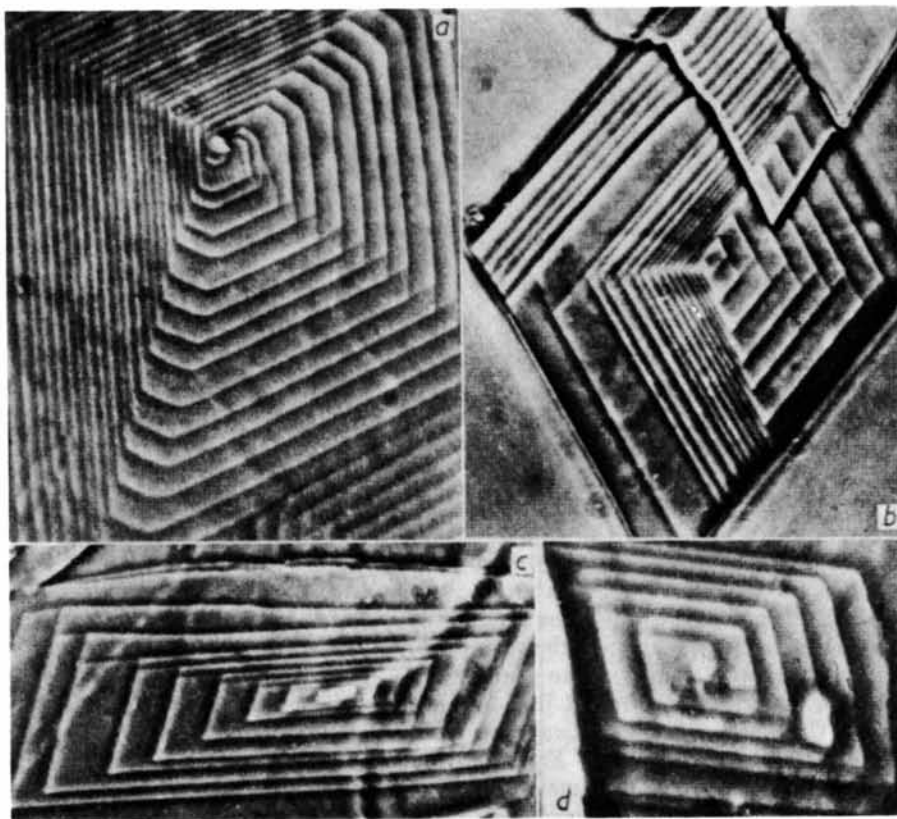


Fig. 13. Simply interlaced spirals on crystals of the  $\alpha$ -form of  $n$ -alcohols.



A further, minor, objection to our analysis might be that the polar diagram is influenced by the substrate when this has an orientation difference of  $180^\circ$  with respect to the normal substrate.

For crystals of the *B*-form of the monocarboxylic acids, where the anisotropy is smallest, we have reasons to say that the influence of the orientation difference is very small, if it exists at all. This follows from the following argument. It is clearly visible that in the centres of the spirals of Figs. 6(a) and 6(b) the fronts are first grouped without interlacing, then dissociate, and finally are grouped in an interlaced way.

It is immediately evident that, when  $v_a$  and  $v_b$  are respectively the velocities of the two fronts, they will join after having developed a number of windings

$$w = v_a/(v_b - v_a) \quad (v_a < v_b).$$

Using for  $v_b/v_a$  the mean value 1.20, one finds  $w = 5$ , in reasonable agreement with the observed value. This proves that the ratio  $v_b/v_a$  has not changed very much for the interlaced spiral. The reason why this change in composition is produced only in one half of the spiral is clearly that the composition in one half of the spiral has necessarily its stable form at the start. This stable form is assumed to be such that the molecules of the lower layer form an acute angle with the basal plane (Fig. 12(b)).

## 6. Polytypism and interlaced spirals on crystals of the $\alpha$ -form of *n*-alcohols

### 6.1. Introduction

Part I was devoted to the polytypism of the  $\beta$ -form of the *n*-alcohols, while in Part II the normal growth patterns associated with perfect dislocations observed on crystals of the  $\alpha$ -form were described.

They consist of interlaced spirals, in most cases of the type shown in Fig. 13(a) and (b). The polar diagram for a monolayer can be deduced only partly from it. It was found, however, that the anisotropy in growth velocity of a monolayer growing on a OH-OH bond can be described by means of the same polar diagram as the growth velocity for a monolayer growing on a CH<sub>3</sub>-CH<sub>3</sub> bond. One diagram can be derived from the other by taking the mirror image of it with respect to the short diagonal of the lozenge (see Fig. 13).

### 6.2. Analysis of interlaced pattern

We sometimes observed also interlaced patterns of the type shown in Fig. 9. Coincidentally, we also found on the same crystal the normal pattern of Fig. 13, so that we are sure about the polar diagram corresponding to the local growth conditions.

There is now 'cross-lacing' in the four 'corners' of the spiral, and the spacings are equal in the four sectors.

Without the exact knowledge of the step height of

the interlacing steps no unambiguous conclusion can be reached as to the stacking of the crystal. We can, however, deduce what kind of stacking fault is responsible for the formation of the polytypic crystal on which the pattern was observed. We therefore simplify the problem, without, however, omitting the essential features. We will suppose that all cross-lacing steps of the same kind are equal and that the lower among them are monomolecular. The pattern can then be decomposed into four monomolecular spirals, as shown in Fig. 14.

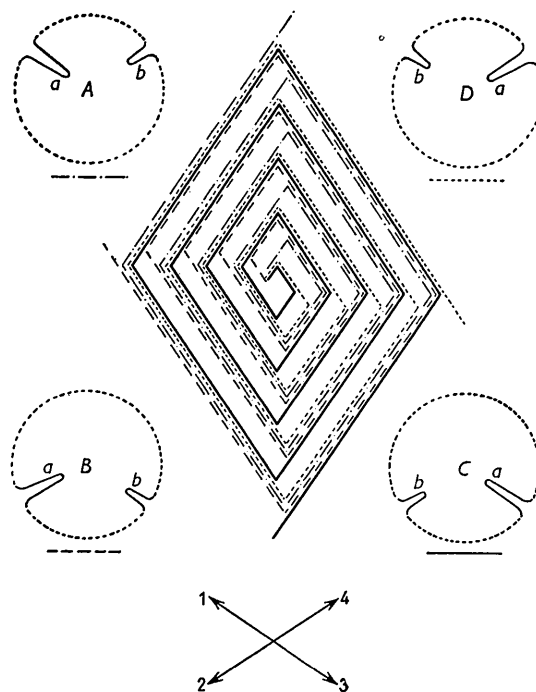


Fig. 14. Decomposition of 'doubly interlaced' spiral observed on a crystal of the  $\alpha$ -form of the *n*-alcohols.

When assuming for the monolayers *A*, *B*, *C* and *D* the polar diagrams in the orientations also indicated in Fig. 14, it is clear that correct interlacing is obtained and that the spacings will be equal in the four sectors. We have in fact postulated that the sets of polar diagrams for successive bimolecular layers are turned over with respect to the following through  $180^\circ$ .

To interpret this result in terms of the crystal structure, a detailed knowledge of it would be necessary. This is, however, lacking for the moment. We can nevertheless explain in a reasonable way the possibility of occurrence of this kind of pattern, and deduce the stacking sequence responsible for it.

Let us consider the limiting surfaces of a bimolecular layer which consist of CH<sub>3</sub> groups (see Fig. 15). The next layer will be put on it in such a way that spheres fit into hollows  $\Delta$  or  $\nabla$ . When the orthorhombic symmetry and a normal *c* periodicity (bimolecular) is to be maintained, all layers must be stacked in such a

way that the spheres come always into the same family of hollows, e.g.  $\Delta$ . In this way the  $\text{CH}_3$  groups of the upper surface of one layer come exactly above the  $\text{CH}_3$  groups of the upper surface of the layer underneath.

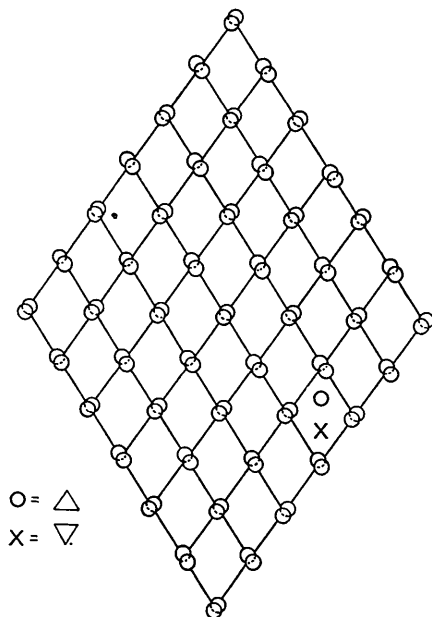


Fig. 15. Limiting surface of  $\text{CH}_3$  groups of orthorhombic long chain crystals.

When, however, layers are placed alternately in a  $\Delta$  and a  $\nabla$  hollow the  $c$ -periodicity will double. Moreover, it is evident from the scheme of Fig. 15 that to a rough approximation the environment of the  $\text{CH}_3$  group in a  $\Delta$  layer is related to the environment of the  $\text{CH}_3$  group in a  $\nabla$  layer by means of a rotation through  $180^\circ$ . The change in stacking can thus be described approximately by a rotation of the layer through  $180^\circ$ . We still accept the principle (Part I) that the orientation of the polar diagram is bound to the orientation of the layer. We then obtain from the set of two polar diagrams for the first bimolecular layer ( $AB$ ), the set of polar diagrams for the second layer ( $CD$ ), the diagrams for  $A$  and  $C$  and for  $B$  and  $D$  being related by the rotation through  $180^\circ$ .

The stacking symbol of the crystal exhibiting the hypothetical simplified spiral pattern of Fig. 14 should

consequently be  $\Delta\nabla$ . The symbols are here stacking operators (Frank, 1951) for bimolecular layers and are to be distinguished from the symbol  $A$ , which represents the layer itself in a given orientation.

We have implicitly accepted that the stacking in the  $\text{OH-OH}$  region is not subject to stacking faults. This is a reasonable assumption, as this bond is polar and stronger than the  $\text{CH}_3\text{-CH}_3$  bond.

We have here described and analysed the first example of what could be called a 'doubly interlaced spiral', i.e. an interlacing of two spiral patterns, which are themselves interlaced.

The author is grateful to Prof. W. Dekeyser for the stimulating interest taken in this work, which is part of a research programme (Centre pour l'étude de l'État Solide) supported by I.R.S.I.A. (Institut pour l'encouragement de la Recherche Scientifique dans l'Industrie et l'Agriculture).

We wish to thank also Prof. Stenhagen, of Upsala University, for a pure sample of the paraffin  $\text{C}_{34}\text{H}_{70}$  and Prof. Dr Govaert and Dr Versele, of Ghent University, for the samples of carboxylic acids and alcohols.

### References

- AMELINCKX, S. (1953). *Naturwissenschaften*, **40**, 620.  
 AMELINCKX, S. (1954). *Naturwissenschaften*, **41**, 356.  
 AMELINCKX, S. (1955). *Acta Cryst.* **8**, 530.  
 AMELINCKX, S. (1956). *Acta Cryst.* **9**, 16.  
 ANDERSON, N. G. & DAWSON, I. M. (1953). *Proc. Roy. Soc. A*, **218**, 255.  
 ANDERSON, N. G., DAWSON, I. M. & WATSON, D. H. (1954). *Naturwissenschaften*, **41**, 211.  
 DAWSON, I. M. (1952). *Proc. Roy. Soc. A*, **214**, 72.  
 DAWSON, I. M. & VAND, V. (1951). *Proc. Roy. Soc. A*, **206**, 555.  
 FRANK, F. C. (1949). *Disc. Faraday Soc.* **5**, 48.  
 FRANK, F. C. (1951). *Phil. Mag.* (7), **42**, 1014.  
 MAZEE, W. M. (1948). *Rec. Trav. chim. Pays-Bas*, **67**, 197.  
 MÜLLER, A. (1928). *Proc. Roy. Soc. A*, **120**, 137.  
 MÜLLER, A. (1932). *Proc. Roy. Soc. A*, **138**, 514.  
 PIPER, S. H., MALKIN, T. & AUSTIN, H. E. (1926). *J. Chem. Soc.* p. 2310.  
 TOLANSKY, S. (1948). *Multiple Beam Interferometry of Surfaces and Thin Films*. Oxford: University Press.  
 VERMA, A. R. (1955). *Proc. Roy. Soc. A*, **228**, 34.  
 VERMA, A. R. & REYNOLDS, P. M. (1953). *Proc. Phys. Soc.* **66**, 414.